Chemistry–A European Journal
Research Article
doi.org/10.1002/chem.202104563
Chemistry Europe
European Chemical Societies Publishing
www.chemeurj.org

Highly Sensitive "Off/On" EPR Probes to Monitor Enzymatic Activity

Sabrina Elkhanoufi,[a] Rachele Stefania,[a] Diego Alberti,[a] Simona Baroni,[a] Silvio Aime,[a] and Simonetta Geninatti Crich*[a]

Abstract: The assessment of unregulated level of enzyme activity is a crucial parameter for early diagnoses in a wide range of pathologies. In this study, we propose the use of electron paramagnetic resonance (EPR) as an easy method to probe carboxylesterase (CE) enzymatic activity in vitro. For this application, were synthesized two amphiphilic, nitroxide containing esters, namely Tempo-C12 (T-C12) and Tempo-2-C12 (T-2-C12). They exhibit low solubility in water and form stable micelles in which the radicals are EPR almost silent, but the hydrolysis of the ester bond yields narrows and intense EPR signals. The intensity of the EPR signals is proportional to the enzymatic activity. CEs1, CEs2 and esterase from porcine liver (PLE) were investigated. The obtained results show that T-C12 and T-2-C12-containing systems display a much higher selectivity toward the CEs2, with a Limit of Detection of the same order of those ones obtained with optical methods.

Introduction

Assessment of enzymatic activity in biological fluids is commonly pursued by means of spectrofluorimetric assays.[1] Although EPR is recognized as a modality characterized by a good sensitivity, it has not yet found widespread application in the field of enzymatic assays. Only in recent years, its potential has been exploited in body fluids in assays designed to test the activity of the following enzymes: elastase,[2,3] alkaline phosphatase,[4] lipases[5] and cathepsin G.[6] The proposed approach invariantly relies on the use of nitroxide-containing substrates that the enzyme transforms into products whose phosphorous hyperfine constant is different from the parent species. This frequency-encoding modality allows an unambiguous detection of the enzymatic product, but the attainable sensitivity level appears until now limited.[5,6] We deemed of interest to investigate alternative routes taking advantage of the fact that nitroxide radicals are "quenched" when they are immobilized on nanostructures like proteins,[7] vesicles, micelles or liposomes[8,9] as a consequence of dipole-dipole interactions and increasing spin exchange between the closely packed radical molecules.[10] In alternative, Lu Yu and coworkers[11] recently observed a significant quenching of the EPR signal generated by the dipolar interaction with a paramagnetic center (Gd-complex) linked through a short protease-specific peptide to the nitroxide radical. Direct detection of caspase-3 activity was possible by analyzing the EPR signal increase upon specific peptide cleavage. The proposed methodology relies on the synthesis of nitroxide-containing lipids in which the spacer between the radical and the aliphatic chain is designed to act as suitable substrate for the enzyme of interest. Upon the enzymatic cleavage, the nitroxide radical becomes free in solution displaying its characteristic triplet pattern in the EPR spectrum. This procedure was already proposed by Audran et al.[5] using different shifting nitroxides with ester bonds. We expect that the proposed "off-on" approach can be of general applicability upon the proper choice of the spacer whose cleavage by a specific enzyme yields free nitroxides radicals. The measurement of their signal intensity reports on the enzymatic activity. Herein we report a proof-of-concept study when the proposed methodology is applied to the assessment of carboxylesterases (CEs) activity. These enzymes, belong to the serine hydrolase superfamily, catalyze the ester hydrolysis of a large number of endogenous substrates such as cholesterol ester, acylcarnitine and many exogenous drugs,[12–15] playing a key role in both cell metabolism, and activation of xenobiotics, in particular cancer pro-drugs.[16,17] CEs are up-regulated in many tumors as pancreatic cancer,[16,18] neuroblastoma,[19] non-small cell lung cancer,[20] and colorectal cancer tissue.[21,22] Thus, the detection of CEs in living systems could improve the diagnosis of the disease, as well as it may provide important information regarding chemotherapeutic effects of antitumor ester drugs and pro-drugs. In humans, the most common CEs are those named CE1 and CE2. CE1 is abundantly expressed in the liver and adipocyte[17,23] whereas CE2 is expressed mainly in the small intestine and colon, but also observed in kidney, liver, heart, brain and testis.[17,24]

Interestingly, a high level of CE1 was found in the blood of patients with hepatocellular carcinoma (HCC).[25] Moreover, it

[a] S. Elkhanoufi, R. Stefania, D. Alberti, S. Baroni, S. Aime, Prof. S. Geninatti Crich
University of Torino
Department of Molecular Biotechnology and Health Sciences
via Nizza 52, 10126, Torino (Italy)
E-mail: simonetta.geninatti@unito.it

Supporting information for this article is available on the WWW under https://doi.org/10.1002/chem.202104563

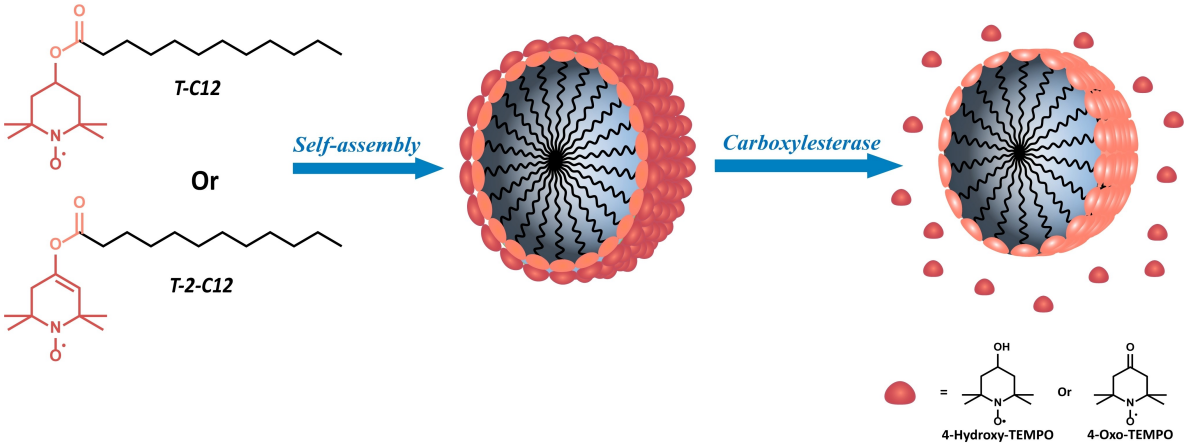

Figure 1. Chemical structure of Tempo-C12 (T-C12) and Tempo-2-C12 (T-2-C12); graphic representation of the micelles obtained with the two compounds and release of the radicals in presence of the CE.

has been recently shown that hepatoma released exosome-like vesicles contain several metabolic enzymes such as esterases.[26] This observation opens interesting possibilities for the development of an EPR based assay for extracellular esterases including those ones present inside the microvescicles thus exploring their role in drug detoxification and tumor promoting properties. In this study, we synthesized two nitroxide acyl esters containing a C12 aliphatic chain, namely Tempo-C12 (T-C12), and Tempo-2-C12 (T-2-C12). These amphiphilic compounds form, in water, stable aggregates that are almost EPR silent. Thus, the enzymatic hydrolysis of the ester bonds of T-C12 and T-2-C12 radicals yield the stable and easily detected 4-hydroxy-tempo (Tempol) or 4-oxo-tempo (Tempone), respectively (Figure 1).

Results and Discussion

Synthesis and characterization of the EPR nitroxide probes

The esterification reaction of tempo derivatives with lauroyl chloride was carried out in a one-step[9] reaction using pyridine as a base and in a two-step process,[4] through enolate formation, using lithium diisopropyl amide (LDA) as a strong base to obtain compound T-C12 and T-2-C12, respectively (Scheme 1). The compounds were obtained in good/moderate yields after purification by silica gel chromatography (74% and 60% respectively).

T-C12 and T-2-C12 form stable aggregates when 50 μL of their acetonitrile solution were diluted in 950 μL of HEPES-Buffered saline at pH 7.4. Dynamic Light Scattering (DLS) measurements showed an average diameter of 202.07 ± 3.62 nm (DPI 0.032 ± 0.015) and 193.60 ± 7.23 nm (DPI 0.025 ± 0.019) for T-C12 and T-2-C12 respectively (Figure S1). The relatively large size of these aggregates may be accounted in terms of the formation of multimicellar aggregates[27,28] as the consequence of the low hydrophilicity of the neutral nitroxide groups. This hypothesis was confirmed by the observation of

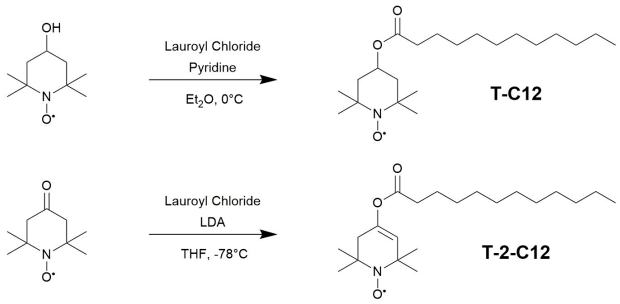

Scheme 1. Synthesis of Tempo-C12 (T-C12) and Tempo-2-C12 (T-2-C12).

smaller sizes upon sonication (58 nm and 52 nm, for T-C12 and T-2-C12 respectively) (Figure S1). However, after 1.5 h the size of the micelles returned to ca. the original value of the non-sonicated ones. Additionally, the zeta potential (ζ) was measured for both the micellar aggregates (T-C12 = +26.7 ± 8.2 mV and T-2-C12 = +19.2 ± 3.8 mV). The positive value is probably due to the presence of a small % of the oxoammonium cations and provide the system with a sufficient stability. The radicals in the micellar aggregates are almost EPR silent showing only a low intensity and broad EPR signal (Figure S2, line width peak to peak 28.7 and 23.9 MHz for T-C12 and T-2-C12, respectively) over all the investigated concentration range (from 10 μM to 500 μM) compared to the signal expected by the free nitroxides (Figure 2A, 2B).

The long-term micellar aggregates stability was assessed in HEPES-Buffered saline at 4 and 25 °C. After 5 days the EPR spectra of the micelles does not exhibit any triplet peaks, associated to the micelle disaggregation or radical hydrolysis (Figure S3). Control samples containing the 4-hydroxy-tempo and 4-oxo-tempo alone left under the same conditions confirmed the maintenance of the radical redox state (Figure S4).

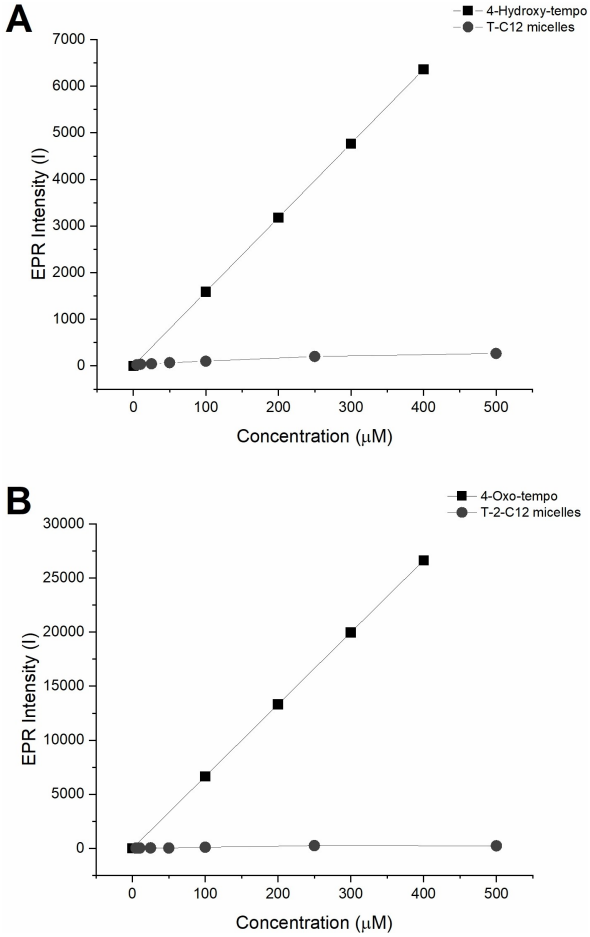

Figure 2. EPR intensity of T-C12 (A) and T-2-C12 (B) micelles at different concentration compared to their corresponding 4-hydroxy-tempo and 4-oxo-tempo radicals.

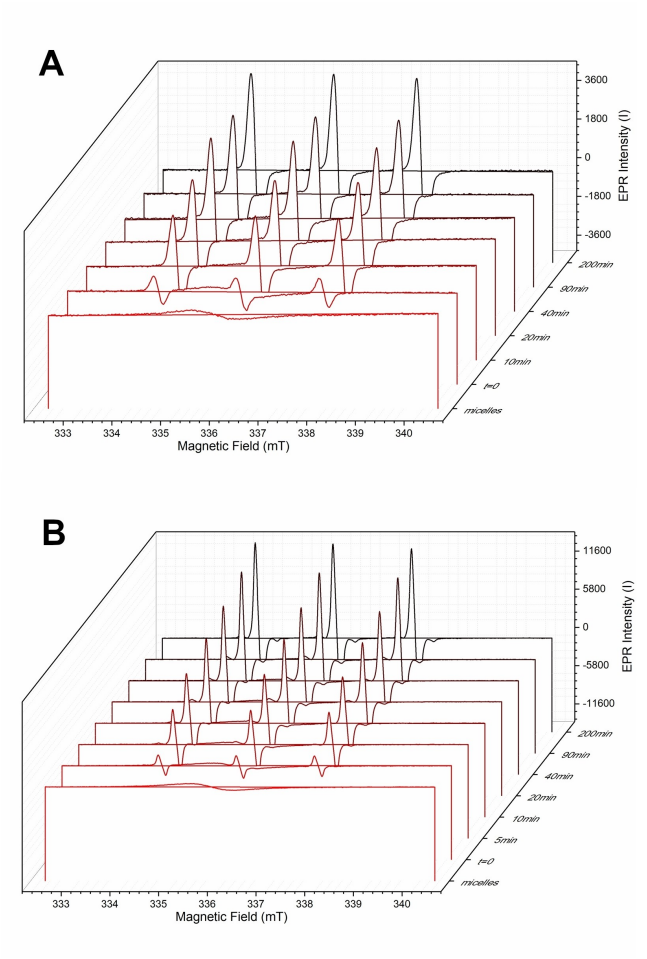

Figure 3. Stack-plots reporting on the time evolution of EPR spectra of T-C12 500 μM (A) and T-2-C12 (B) containing micelles (500 μM in terms of monomer concentration) in HEPES-Buffered saline aqueous solution upon incubation at 37 °C with PLE 61 nM from 0 to 200 minutes.

Enzymatic hydrolysis by esterases

The ability of T-C12 and T-2-C12 micelles to act as a substrate for esterases was tested, at first, with Porcine Liver Esterase (PLE). Figure 3 shows that starting from an almost completely silent EPR response at t = 0, then PLE catalyzed the hydrolysis of T-C12 and T-2-C12 yielding a narrow EPR triplet signal due to the release of the nitroxide radicals from the micelles, whose intensity is proportional to the PLE hydrolytic activity. Upon comparing the enzymatic hydrolysis of the two micelles, at the same enzyme (PLE) concentration, the EPR signal observed after the hydrolysis of T-2-C12 was significantly higher (Figure 4A).

The observed behavior can be accounted in terms of some specificity associated to the mixture of esterases present in PLE as well as a contribution that may arise from the narrower peaks of the more rigid product 4-oxo-tempo (Figure S5, line width peak to peak 5.37 and 4.31 MHz for 4-hydroxy-tempo and 4-oxo-tempo, respectively).[29] Interestingly, the EPR signal observed 24 h after enzymatic hydrolysis remained the same observed after 3 h, thus confirming the high stability of the nitroxide radicals (Figure S6). The enzymatic assay was then carried out in the presence of human carboxylesterases CE1 s and CE2 s, respectively. The obtained results showed that T-C12 is selectively hydrolyzed only by CEs2 (Figure 4B) whereas T-2-C12 is hydrolyzed by both enzymes with CEs2 displaying a much higher efficiency (Figure 4B). This is likely due to the fact that the preferred substrates for CEs1 are systems with smaller alcohol-derived groups, with low steric hindrance, and bulky acyl groups.[17] Other hydrolases and proteins such as HSA, BSA, Human Serum, Lysozyme, Trypsin, Protease and Phospholipase A2 (PLA2) were also investigated without observing any detectable hydrolyzing capacity on the two compounds considered in this work (Figure 5).

Enzymatic kinetics

To study the enzymatic kinetics CEs1 and CEs2 were incubated with the two EPR-responsive probes at different concentration. The plot of the EPR signal intensities showed a sigmoidal shape, so they fitted better with the Hill equation instead of the hyperbolic plot of the Michaelis-Menten equation, showing that

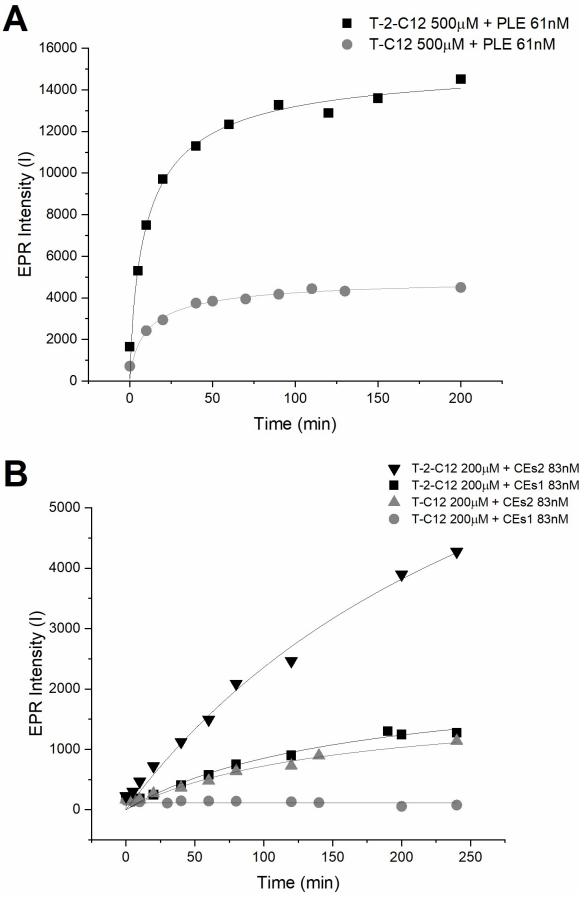

Figure 4. A) EPR signal intensity of T-C12 500 μM (gray curve) and T-2-C12 500 μM (black curve) incubated with PLE 61 nM from 0 to 200 minutes; B) EPR signal intensity of T-C12 200 μM (gray curve) and T-2-C12 200 μM (black curve) incubated with CEs1 and CEs2 83 nM at 37 °C from 0 to 240 minutes.

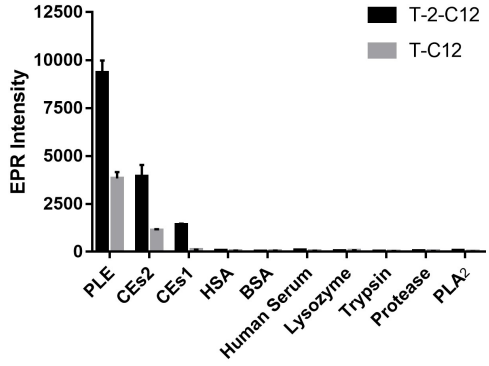

Figure 5. Selectivity assays of T-C12 and T-2-C12 200 μM with HSA, BSA, Lysozyme, Trypsin, Protease and PLA2 83 nM and Human serum (0.01 % dilution in HEPES-Buffered saline aqueous solution) incubated for 3 h at 37 °C.

the enzyme has an allosteric site (Figure 6).[30] The Hill coefficient values obtained from the fitting procedure resulted to be >1 to indicate a positive cooperativity in the presence of the substrates (Figure S7-S9). The kinetic constants listed in the Table 1 show that T-2-C12 has a slightly lower affinity (K_m)

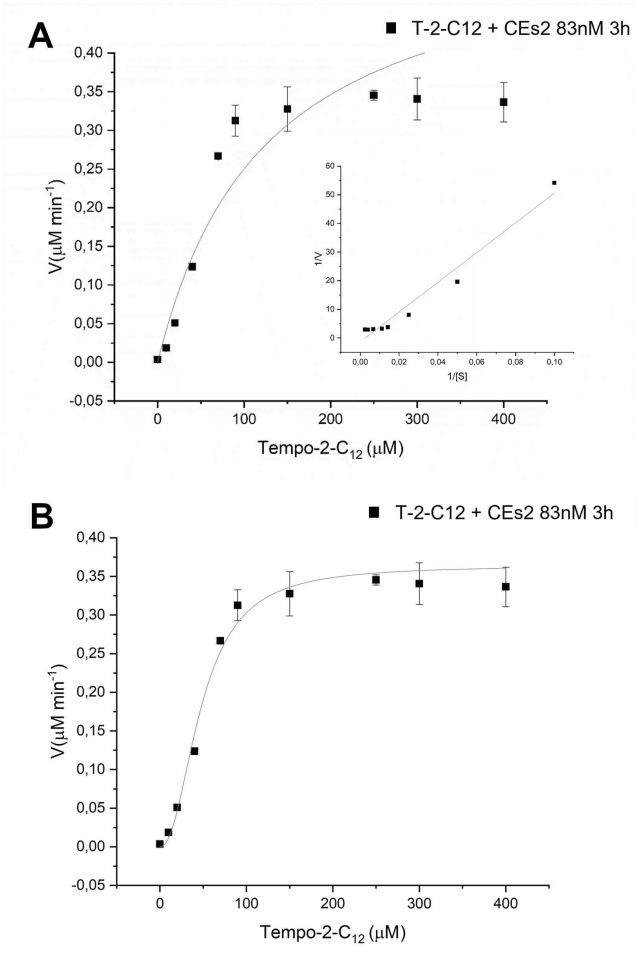

Figure 6. Enzymatic Kinetics of CEs2 83 nM with T-2-C12 incubated for 3 h at 37 °C. Figure 6A shows the results fitted with the Michaelis-Menten equation and the Lineweaver–Burk plot, Figure 6B the fitting with the Hill equation.

Table 1. Kinetic constants calculated from the fitting of T-C12 and T-2-C12 with CEs1 and CEs2.

Enzyme	V_{max} [μM min^{-1}]	K_m [μM]	k_{cat} [min^{-1}]	k_{cat}/K_m [M^{-1} min^{-1}]
T-2-C_{12} + CEs1	0.18 ± 0.012	36.92 ± 4.92	2.17 ± 0.14	5.88×10^4
T-2-C_{12} + CEs2	0.36 ± 0.023	48.07 ± 4.29	4.34 ± 0.28	9.03×10^4
T-C_{12} + CEs2	0.43 ± 0.03	38.31 ± 5.13	5.18 ± 0.36	1.35×10^5

(−23 %) towards CEs2 in respect to CEs1, but the turnover number (k_{cat}) and the catalytic efficiency (k_{cat}/K_m) are significantly higher for CEs2 (+100 %). Moreover, T-C12 displayed both a slightly higher affinity for CEs2 with respect to the T-2-C12 (+25 %) and a higher k_{cat} and catalytic efficiency (+19 %) for this enzyme, which is probably due to the higher selectivity of T-C12.

Limit of detection (LoD)

The limits of detection were estimated by adding to T-C12 and T-2-C12 containing micelles solutions, different concentrations of PLE or CEs and measuring the EPR signal intensities upon time. The observed signal intensities displayed a linear increase (Figure 7).The explored range of concentrations was 0–0.013 U/mL for the T-C12 and 0–0.0032 U/mL for T-2-C12, with PLE and 0–2.49 U/mL with CEs, respectively. The LoD was calculated using the Equation $\boldsymbol{LoD} = \frac{3\sigma}{m}$ where σ is the SD of the blank and m is the slope of linear fitting of data in the linear range (Figure S10-S13). The detection limits obtained (Table 2) with PLE were 2.33×10^{-5} U/mL and 8.00×10^{-5} U/mL, while with CEs2 were 7.06×10^{-2} U/mL and 2.04×10^{-2} U/mL for T-C12 and T-2-C12, respectively (Figure 7). The obtained results are of the same order of magnitude of those ones achievable with optical methods[31–34] (Table S1) thus confirming the high performance of EPR as a highly sensitive technique for the development of competitive enzymatic assays.

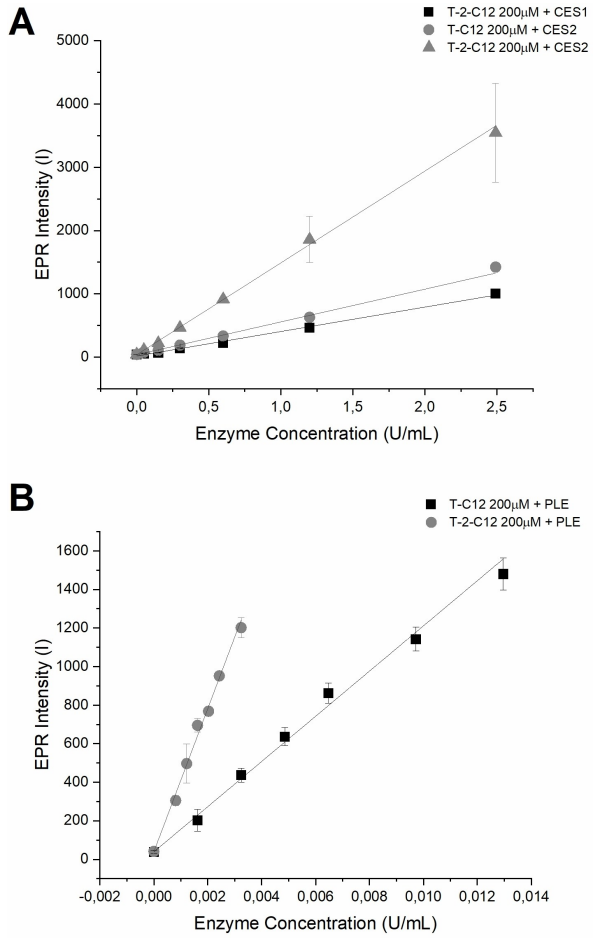

Figure 7. Linear regression of EPR signal intensity after 3 h of incubation at different enzyme concentrations in HEPES buffer. A) T-C12 200 μM and T-2-C12 200 μM with CEs2 (gray lines) and CEs1 (black line); B) T-C12 200 μM (black line) and T-2-C12 200 μM (gray lines) with PLE.

Table 2. LoD results obtained with T-C12 and T-2-C12 micelles with PLE and CEs.

Probe	Method	LoD [U/mL] CEs1	CEs2	PLE
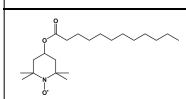	EPR	/	7.06×10^{-2}	2.33×10^{-4}
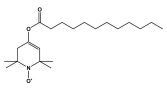	EPR	5.73×10^{-2}	2.04×10^{-2}	8.00×10^{-5}

Conclusions

The results reported in this study demonstrated that EPR detection of stable radicals is an easy and reliable method that reaches the same performance of fluorescent probes without any interference coming from the background. Tempo- based radicals can be easily functionalized with aliphatic chains through, for example, the insertion of esters, phosphoesters, or amidic bond that can be the substrate of different classes of enzymes that act as biomarkers for the early detection of different pathologies or as reporters of therapeutic treatments. One of the advantages of these EPR probes relies also in their easy preparation and purification when compared to the related shifting nitroxide compounds. The "off-on" transition makes the methodology extremely sensitive and quantitative avoiding the use of complex ratiometric corrections to eliminate the contribution arising from the not hydrolyzed probes. In fact, the obtained sensitivity (8.00×10^{-5} U/mL) is of the same order of magnitude of the values achieved with optical methods and is significantly enhanced with respect the use of shifting nitroxides, labeled with fatty acids, that split the EPR signal in 6 instead of 3.[5] Finally, the method has the potential to be translated to in vivo applications via OMRI (Overhauser Magnetic Resonance Imaging) protocols.[2–6,35–37] For this application, the use of probes characterized by narrow EPR signals is crucial to provide high sensitivity and specificity in the polarization transfer from electrons to water protons. Although, the stability and efficacy of T-C12 and T-2-C12 under in vivo conditions have not yet been assessed, they can be certainly improved by the substitution of the 6-membered ring nitroxides with the more stable 5-membered proxyl derivatives. This would give the chance for the in vivo detection of specific enzymatic activities by OMRI using these Off/On probes.

Experimental Section

Materials and instrumentation

All the compounds were purchased at Sigma-Aldrich, Human serum (Seronorm Human) from Sero, all the solvent from VWR. The characterization by HPLC-UV-MS(ESI+) was done on a Waters system (3100 Mass Detector, 2525 quaternary pump, 2767 sample manager, 2996 PDA detector). HPLC-HRMS(ESI+) used for further characterization was a Thermo Fisher system (Thermo Dionex 3000, Thermo Orbitrap Fusion). 1H NMR and 13 C NMR on NMR Bruker Avance 600 MHz spectrometer. EPR spectra were acquired with

Adani EPR spectrometer Spinscan × (9.2–9.55 GHz) using as parameters: center field = 336.50 mT, sweep width = 8 mT, sweep time = 30 s, modulation amplitude = 150 uT, attenuation = 20 dB, temperature = 25 °C. All the enzymatic incubation were done in Starlab Thermomixer-Mixer HC at 37 °C and 400 rpm. For the sonication of the micelles the Sonicator Bandelin Sonoplus HD 2070 was used. The dimensions were determined using dynamic light-scattering (Malvern ZS Nanosizer, UK) and reported as number-weighted average size.

Synthesis

Tempo-C12 *(4-Decanoyloxytempo)* ***(1)***: In a dried 50 mL round-bottom flask 4-hydroxy-tempo (2 mmol, 0.34 g) and pyridine (5.5 mmol, 0.44 mL) were dissolved in 8 mL of anhydrous diethyl ether (Et_2O). The mixture was cooled at 0 °C and lauroyl chloride (5.5 mmol, 0.44 mL) diluted in anhydrous Et2O was added dropwise, the solution was then stirred for 24 h at room temperature. Afterward the mixture was filtered, concentrated under vacuum and purified by column chromatography on silica gel (n-hexane/diethyl ether 8.5:1.5), to obtain Tempo-C12 (1) (0.53 g, 74% yield) as an orange solid. 1H NMR (600 MHz, DMSO-*d6*, Phenylhydrazine) δ (ppm): 4.95 (1H, m, J1 = 4.2 and J2 = 7.2, CH), 3.92 (1H, s, NOH), 2.25 (2H, t, J = 7.2, CH_2CO), 1.97 (2H, dd, J1 = 1.8, J2 = 9, CHeq), 1.51 (2H, m, CH_2), 1.43 (2H, m, J = 12, CHax), 1.25 (16H, s, CH_2), 1.09 (6H, s, CH_3), 1.08 (6H, s, CH3), 0.88 (3H, t, CH3). 13 C NMR (150 MHz, DMSO-*d6*, Phenylhydrazine) δ (ppm): 172.21, 65.85, 57.71, 43.44, 33.50, 31.85, 31.02, 28.69, 28.66, 28.54, 28.43, 28.32, 28.07, 24.20, 21.82, 20.17, 13.71.

The purity of the isolated compounds (> 95%) was determined with a HPLC-UV-MS (ESI+) analysis using Xterra Phenyl column, 5 μm, 4.6 mm × 150 mm, applying a gradient of CH_3CN (0.1% TFA) in H2O (0.1% TFA) from 50% to 70% in 5 min and from 70% to 100% in 25 min (1 mL min^{-1}) (retention time 8.3 min). MS (ESI+): m/z: calcd for $C_{21}H40NO3^{\bullet}$: M+ oxoammonium cation 354.3 (obsd.) 354.3 calcd, [M+H]+ •355.3 (obsd) 355.3 calcd, [M+H2]+ 356.4 (obsd) 356.3 calcd, [M-14]+340.3 (obsd) 340.3 calcd. The exact mass was confirmed with a HRMS: [M+H]+ • 355.3078 (obsd) 355.3081 calcd. See Supporting Information Figure S14 for 1H NMR, Figure S15 for ^{13}C NMR, Figure S16 for HPLC-UV-ESI-MS and Figure S17 for HRMS.

Tempo-2-C12 *(4-Decanoyloxy-3-en-tempo)* ***(2)***: In a dried 50 mL round-bottom flask 4-oxo-tempo (1 mmol, 0.17 g) was dissolved in THF (6 mL) and cooled at −78 °C. Lithium diisopropylamide (LDA) (1.5 mmol, 1.5 mL, 1 M) was added dropwise and the reaction was stirred for 2 h at −78 °C. Then lauroyl chloride (2 mmol, 0.45 mL) was added and the solution was stirred for 1 h at −78 °C and at room temperature overnight. The solution was quenched with a saturated solution of ammonium chloride sat. (10 mL), extracted with EtOAc (2 × 5 mL), dried with MgSO4 and concentrated under vacuum. The crude was then purified by silica gel column chromatography (n-hexane/ethyl acetate = 9:1) to obtain Tempo-2-C12 (**2**) (0.16 g, 57%) as an orange solid. 1H NMR (600 MHz, DMSO-d6, Phenylhydrazine) δ (ppm): 5.23 (1H, s, CH), 2.36 (2H, t, J = 7.2, CH2CO), 2.13 (2H, s, CH2), 1.55 (2H, m, J = 6.6, CH_2), 1.26 (16H, m, CH_2), 1.17 (6H, s, CH3), 1.12 (6H, s, CH3), 0.87 (3H, t, J = 7.2, CH_3). 13 C NMR (150 MHz, DMSO-d6, Phenylhydrazine) δ (ppm): 171.07, 142.19, 116.39, 57.80, 57.06, 40.73, 33.15, 31.03, 28.71, 28.70, 28.55, 28.45, 28.33, 28.06, 24.05, 21.83, 13.65.

The purity of the isolated compounds (> 95%) was determined with a HPLC-UV-MS (ESI+) analysis using Xterra Phenyl column, 5 μm, 4.6 mm × 150 mm, applying a gradient of CH3CN (0.1% TFA) in H2O (0.1% TFA) from 50% to 70% in 5 min and from 70% to 100% in 25 min (1 mL min-1) (retention time 8.41 min). MS (ESI+): m/z: calcd for calcd for $C21H38NO3^{\bullet}$: M+ oxoammonium cation 352.3 (obsd.) 352.3 calcd, [M+H]+ • 353.3 (obsd) 355.3 calcd, [M+H2]+ 354.3 (obsd) 354.3 calcd, [M-14]+338.3 (obsd) 338.3 calcd. The exact mass was confirmed with a HRMS: [M+H]+ • 353.2928 (obsd) 353.2924 calcd. See Supporting Information Figure S18 for 1H NMR, Figure S19 for 13 C NMR, Figure S20 for HPLC-UV-ESI-MS and Figure S21 for HRMS.

Preparation of the micelles: The micelles were obtained by dissolving T-C12 or T-2-C12 in acetonitrile at different concentration from 200 μM to 20 mM. Then 50 μL of these solutions were added to 950 μL of HEPES-Buffered saline (pH 7.4, 3.8 mM of HEPES, 0.15 M of NaCl) and vortexed. Prior the DLS measurements the solutions were sonicated for 5 min, 2 cycle (0.2 sec. on and 0.8 sec. off) at 70% of power and during sonication the solutions were cooled with ice.

Enzyme hydrolysis and selectivity assay: To assess enzymatic activities 50 μL of T-C12 or T-2-C12 10 mM was dissolved in 940 μL of HEPES-Buffered saline aqueous solution, then was added 10 μL of PLE 6.1 μM. The solution obtained, with micelles at 500 μM and PLE 61 nM, were incubated for 200 min at 37 °C. The assay with the CEs was done in the same way but with a final concentration of 200 μM for the micelles and 83 nM for CEs1 and CEs2. During the incubations, 30 μL of the hydrolyzed mixtures was subtracted from the solutions at different times (from 0 to 200 min) for the EPR acquisition. The selectivity assay was done by incubating T-C12 or T-2-C12 200 μM in HEPES-Buffered saline aqueous solution with CEs1, CEs2, PLE, HAS, BSA, Lysozyme, Trypsin, Protease, PLA2 at 83 nM and Human Serum diluted with HEPES-Buffered saline at 0.01%. After 3 h little aliquot was subtracted from the solutions for the EPR acquisition. Each experiment was repeated three times and the data are presented as mean ± SD.

LOD measurements: The limits of detections were estimated by incubating at 37 °C T-C12 and T-2-C12 200 μM micelles and the enzymes for 3 and 6 h. The range of concentration investigated with PLE is 0–0.013 U/mL for the T-C12 and 0–0.0032 U/mL for T-2-C12, while with CEs 0–2.49 U/mL for both micelles. After incubation time a small aliquot was subtracted for the EPR measurement. Each experiment was repeated three times. From the EPR intensities obtained were calculated the mean ± SD, the linear regression of each enzyme and the slope was used to calculate the LOD using the Equation LOD = 3σ/m. The deviation standard of the blank was obtained by measuring 5 different solutions of T-C12 and T-2-C12 200 μM in HEPES-Buffered saline after incubation for 3 and 6 h.

Michaelis-Menten enzyme kinetics assays: The assay was conducted with fixed CEs1 and CEs2 concentration of 83 nM and a concentration range of T-C12 and T-2-C12 micelles from 0 to 400 μM. After 3 h an aliquot was taken for the EPR measurement and each experiment was repeated three times. The mean of the EPR intensities were converted to rates of product formation in minutes (μM min^{-1}) calculated with a calibration curve of the two products (4-hydroxy-tempo and 4-oxo-tempo). The nonlinear regression analysis and the Equation kinetic parameters were calculated with OriginPro 2018. The fitting models used are the Michaelis-Menten Equation $\boldsymbol{V} = \frac{V_{max}[S]}{K_m+[S]}$ and for the Hill Equation $\boldsymbol{V} = \frac{V_{max}x^n}{k^n+x^n}$. For the linearization of the Michaelis-Menten was used the Lineweaver-Burk Equation.

Acknowledgements

This project has received funding from the European Union's Horizon 2020 research and innovation programme under grant agreement No 86309, Primogaia project. Open Access Funding

provided by Universita degli Studi di Torino within the CRUI-CARE Agreement.

Conflict of Interest

There are no conflicts to declare.

Data Availability Statement

Research data are not shared.

Keywords: carboxylesterase · enzymatic activity · EPR spectroscopy · micelles · nitroxide radicals

[1] Y. Ou, R. E. Wilson, S. G. Weber, *Annu. Rev. Anal. Chem.* **2018**, *11*, 509–533.
[2] N. Jugniot, I. Duttagupta, A. Rivot, P. Massot, C. Cardiet, A. Pizzoccaro, M. Jean, N. Vanthuyne, J.-M. Franconi, P. Voisin, G. Devouassoux, E. Parzy, E. Thiaudiere, S. R. A. Marque, A. Bentaher, G. Audran, P. Mellet, *Free Radical Biol. Med.* **2018**, *126*, 101–112.
[3] G. Audran, L. Bosco, P. Brémond, J.-M. Franconi, N. Koonjoo, S. R. A. Marque, P. Massot, P. Mellet, E. Parzy, E. Thiaudière, *Angew. Chem. Int. Ed. Engl.* **2015**, *54*, 13379–13384.
[4] U. Sanzhaeva, X. Xu, P. Guggilapu, M. Tseytlin, V. V. Khramtsov, B. Driesschaert, *Angew. Chem. Int. Ed.* **2018**, *57*, 11701–11705; *Angew. Chem.* **2018**, *130*, 11875–11879.
[5] G. Audran, S. Jacoutot, N. Jugniot, S. R. A. Marque, P. Mellet, *Anal. Chem.* **2019**, *91*, 5504–5507.
[6] I. Duttagupta, N. Jugniot, G. Audran, J.-M. Franconi, S. R. A. Marque, P. Massot, P. Mellet, E. Parzy, E. Thiaudière, N. Vanthuyne, *Chem. Eur. J.* **2018**, *24*, 7615–7619.
[7] P. Mellet, P. Massot, G. Madelin, S. R. A. Marque, E. Harte, J.-M. Franconi, E. Thiaudière, *PLoS One* **2009**, *4*, e5244.
[8] C. Aliaga, M. C. Rezende, G. Mena, *Magn. Reson. Chem.* **2016**, *54*, 870–873.
[9] C. Aliaga, F. Bravo-Moraga, D. Gonzalez-Nilo, S. Márquez, S. Lühr, G. Mena, M. C. Rezende, *Food Chem.* **2016**, *192*, 395–401.
[10] K.-P. Moll, R. Stößer, W. Herrmann, H.-H. Borchert, H. Utsumi, *Pharm. Res.* **2004**, *21*, 2017–2024.
[11] L. Yu, A. Liu, B. Zhang, J. Kuang, X. Guo, C. Tian, Y. Lu, *Chem. Commun.* **2021**, *57*, 9602–9605.
[12] B. L. Barthel, Z. Zhang, D. L. Rudnicki, C. D. Coldren, M. Polinkovsky, H. Sun, G. G. Koch, D. C. F. Chan, T. H. Koch, *J. Med. Chem.* **2009**, *52*, 7678–7688.
[13] V. Charasson, R. Bellott, D. Meynard, M. Longy, P. Gorry, J. Robert, *Clin. Pharmacol. Ther.* **2004**, *76*, 528–535.
[14] L. D. Hicks, J. L. Hyatt, S. Stoddard, L. Tsurkan, C. C. Edwards, R. M. Wadkins, P. M. Potter, *J. Med. Chem.* **2009**, *52*, 3742–3752.
[15] S. E. Pratt, S. Durland-Busbice, R. L. Shepard, K. Heinz-Taheny, P. W. Iversen, A. H. Dantzig, *Clin. Cancer Res.* **2013**, *19*, 1159–1168.
[16] K. Kailass, O. Sadovski, M. Capello, Y. Kang, J. B. Fleming, S. M. Hanash, A. A. Beharry, *Chem. Sci.* **2019**, *10*, 8428–8437.
[17] D. Wang, L. Zou, Q. Jin, J. Hou, G. Ge, L. Yang, *Acta Pharm. Sin. B* **2018**, *8*, 699–712.
[18] M. Capello, J. F. Fahrmann, M. V. Rios Perez, J. V. Vykoukal, E. Irajizad, S. C. Tripathi, D. Roife, L. E. Bantis, Y. Kang, D. L. Kundnani, H. Xu, L. R. Prakash, J. P. Long, H. Katayama, A. Fleury, S. Ferri-Borgogno, D. L. Baluya, J. B. Dennison, C. Aguilar-Bonavides, J. P. Casabar, M. Celiktas, K.-A. Do, O. Fiehn, A. Maitra, H. Wang, Z. Feng, P. J. Chiao, M. H. Katz, J. B. Fleming, S. M. Hanash, *JCO Precis. Oncol.* **2020**, 426–436.
[19] K. Uchida, K. Otake, K. Tanaka, K. Hashimoto, S. Saigusa, K. Matsushita, Y. Koike, M. Inoue, M. Ueeda, Y. Okugawa, Y. Inoue, Y. Mohri, M. Kusunoki, *J. Pediatr. Surg.* **2013**, *48*, 502–509.
[20] K. Ohtsuka, S. Inoue, M. Kameyama, A. Kanetoshi, T. Fujimoto, K. Takaoka, Y. Araya, A. Shida, *Lung Cancer* **2003**, *41*, 187–198.
[21] Y. Zhang, L. Sun, Y. Sun, Y. Chen, X. Wang, M. Xu, P. Chi, Z. Xu, X. Lu, *Experim. Cell Res.* **2020**, *389*, 111856.
[22] C. Shaojun, H. Li, H. Haixin, L. Guisheng, *Cancer Biol. Ther.* **2018**, *19*, 153–159.
[23] S. P. Sanghani, P. C. Sanghani, M. A. Schiel, W. F. Bosron, *Protein Pept. Lett.* **2009**, *16*, 1207–1214.
[24] M. Taketani, M. Shii, K. Ohura, S. Ninomiya, T. Imai, *Life Sci.* **2007**, *81*, 924–932.
[25] K. Na, E.-Y. Lee, H.-J. Lee, K.-Y. Kim, H. Lee, S.-K. Jeong, A.-S. Jeong, S. Y. Cho, S. A. Kim, S. Y. Song, K. S. Kim, S. W. Cho, H. Kim, Y.-K. Paik, *Proteomics* **2009**, *9*, 3989–3999.
[26] J. Conde-Vancells, E. Gonzalez, S. C. Lu, J. M. Mato, J. M. Falcon-Perez, *Expert Opin. Drug Metab. Toxicol.* **2010**, *6*, 543–554.
[27] F. Qiu, Y. Huang, X. Zhu, *Macromol. Chem. Phys.* **2016**, *217*, 266–283.
[28] M. Qi, Y. Zhou, *Mater. Chem. Front.* **2019**, *3*, 1994–2009.
[29] J. Hunold, J. Eisermann, M. Brehm, D. Hinderberger, *J. Phys. Chem. B* **2020**, *124*, 8601–8609.
[30] E. V. Emelyanova, *JBBS* **2018**, *1*, 94–99.
[31] S.-Y. Liu, R.-Y. Qu, R.-R. Li, Y.-C. Yan, Y. Sun, W.-C. Yang, G.-F. Yang, *Anal. Chem.* **2020**, *92*, 9205–9213.
[32] X.-Y. Zhang, T.-T. Liu, J.-H. Liang, X.-G. Tian, B.-J. Zhang, H.-L. Huang, X.-C. Ma, L. Feng, C.-P. Sun, *J. Mater. Chem. B* **2021**, *9*, 2457–2461.
[33] J. Wang, Q. Chen, N. Tian, W. Zhu, H. Zou, X. Wang, X. Li, X. Fan, G. Jiang, B. Z. Tang, *J. Mater. Chem. B* **2018**, *6*, 1595–1599.
[34] S. Kim, H. Kim, Y. Choi, Y. Kim, *Chem. Eur. J.* **2015**, *21*, 9645–9649.
[35] P. Massot, E. Parzy, L. Pourtau, P. Mellet, G. Madelin, S. Marque, J.-M. Franconi, E. Thiaudiere, *Contrast Media Mol. Imaging* **2012**, *7*, 45–50.
[36] D. E. J. Waddington, M. Sarracanie, N. Salameh, F. Herisson, C. Ayata, M. S. Rosen, *NMR Biomed.* **2018**, *31*, e3896.
[37] A. Rivot, N. Jugniot, S. Jacoutot, N. Vanthuyne, P. Massot, P. Mellet, S. R. A. Marque, G. Audran, P. Voisin, M. Delles, G. Devouassoux, E. Thiaudiere, A. Bentaher, E. Parzy, *ACS Omega* **2021**, *6*, 15012–15016.

Manuscript received: December 23, 2021
Accepted manuscript online: February 17, 2022
Version of record online: March 3, 2022